MAPPING OF POLLUTION-SENSITIVE AREAS BY THE PAPRI METHOD, VERIFIED BY NITRATE CONCENTRATIONS IN THE BAYA WATERSHED (EASTERN IVORY COAST).

Manuscript Info

……..

Manuscript History
Received: xxxxxxxxxxxxxxx
Final Accepted: xxxxxxxxxxx
Published: xxxxxxxxxxxxxxx

Key words:
Mapping, vulnerability to pollution, Nitrate, Baya watershed

Abstract

……

Assessment of the quality of groundwater in the Baya watershed in eastern Côte d'Ivoire is important to ensure sustainable and safe use for human consumption. The research objective is to map the areas susceptible to pollution by the PaPRI method. This multi-criteria analysis integrated into the GIS allowed to identify areas susceptible to pollution of the basin with a 95% confidence level. The Baya watershed has a high predisposition to pollution with a cumulative of 57% of the strong and very strong vulnerabilities classes.
The projection of water points on the pollution susceptibility map gave a coincidence rate of 81.13%. This data is an important source of essential information in that it allows a clear picture to be made of the areas sensitive to pollution with a view to taking the necessary protective measures.

……..

Introduction:

Groundwater pollution problems are currently a source of concern requiring universal attention (Amharref et al., 2007). This pollution, generated by anthropogenic activities and geogenic factors (Tekam et *al*., 2019) can, by reaching critical levels, pose a serious danger to public health (Dovonou et *al.*, 2017). According to UNICEF Côte d'Ivoire (2017), drinking water is available to only 81% of the population, 92% of whom live in urban areas and 8% in rural areas.In the Gontougo region, the quality of groundwater that was once dependent on water-submerger interactions (Mangoua, 2013; Youan Ta et *al.*, 2015). Today, this groundwater could be subject to pollution due to anthropogenic activities related to fertilizers and phytosanitary products used by farmers and ranchers to improve their production. The work of Aké (2012) and Blé (2016) reported on this pollution in the Bondoukou, Bonoua and Agboville regions, located in the east and south of Côte d'Ivoire.In addition, the lack of education of the population about the protection of this resource leads to the generation of polluting elements that could modify the chemical parameters of the water (Humphries et *al.*, 2017; Wang et *al.*, 2017) and present a potential risk to human health, livestock farming and aquatic ecosystems in particular (Tekam et *al.*, 2019). Thus, in the face of the difficulties associated with depollution techniques and the cost thereof, protection is required first and foremost by a better knowledge of the mapping of the zones vulnerable to pollution. Providing a clear picture of pollution sensitive areas with a view to taking the necessary protective measures.

I. Materials and Methods

I.1. Study Area Presentation and Location

The Baya watershed is located in eastern Côte d'Ivoire between longitudes 2°38' and 3°33' W and latitudes 6°35' and 8°26' N. It covers an area of approximately 6,324 km2 (Figure 1). The population of the basin is estimated at 267,263 inhabitants with an increase of 2.8% of the population (INS, 2014)as illustrated in Figure 1.
From a soil point of view, this basin is covered with ferralitic soils occupied by cash and export crops (coffee, cocoa, cashew) and food crops (Yves et *al.*, 1995). The main geological formations encountered can be grouped into three large lithological ensembles (Youan Ta et *al.*, 2015). A Tarkwaian and volcano-sedimentary ensemble consisting mainly of Shale, Amphibolite and Metadolerite. From a hydrogeological point of view, there are two types of aquifers in the study area. These are the aquifers of alterites, the aquifers of cracks and fractures. This

hydrogeological framework means that water resources are mainly used for drinking water supply and for hydroelectric production, hence a basin characterized mainly by rainfed agriculture subject to climatic hazards (http://www.water.gov.ma/).

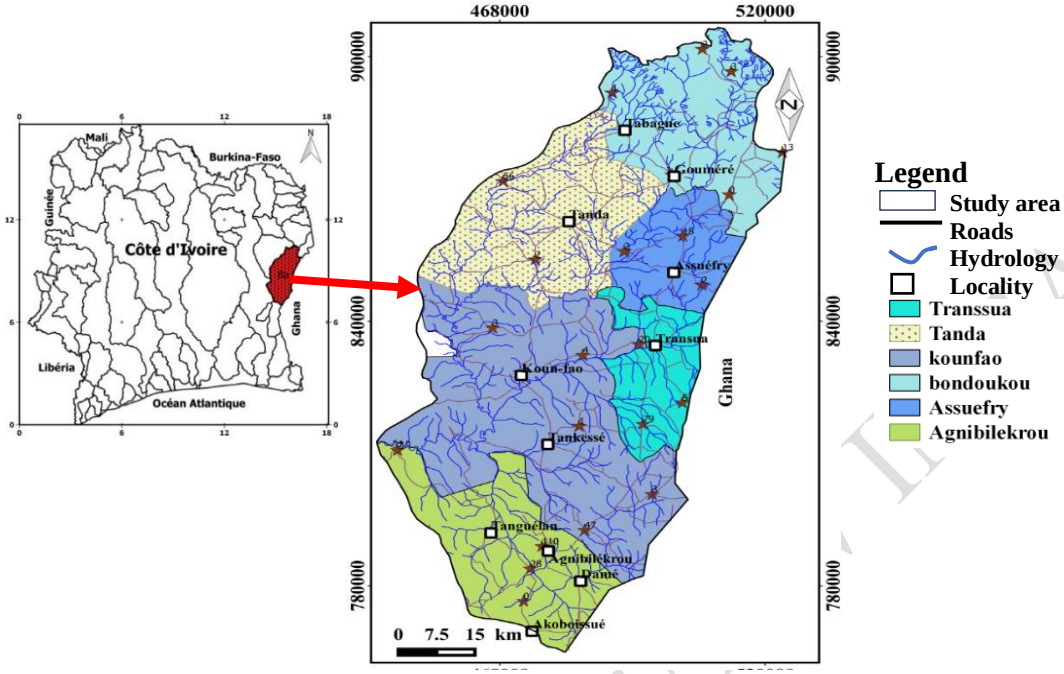

Figure 1 : Study area

I.2. Determination of the overall vulnerability index

The superimposition of the different layers through the GIS makes it possible to obtain a map of vulnerability to pollution of the Baya watershed. The calculation of the overall vulnerability index is based on the DISCO method (SAEFL/SAEFL, 2003), according to the equation (1)

$$Vg = iI + pP + rR \qquad Eq(1)$$

I, P and R represent the various criteria and i, r and pare the weights of these criteria. The weighting coefficients or weights of the criteria P, R and I are calculated from the Saaty pair comparison method (Table 1), an example of which is given in Appendix 7. The analysis of these combinations allowed to establish the limits of the risk classes: 1 (blue) = low risk index; 2 (green) = medium risk index; 3 (yellow) = high risk index; 4 (red) = very high-risk index.

Table1: Summary of weighting coefficients

Scenarios : Protection (P) > Infiltration (I) > Rock (R)

	Protection	Infiltration	Rock	Clean Vector	CP
Protection	1	7	5	3,27	0.71
Infiltration	1/7	1	1/5	0,30	0.06
Rock	1/5	5	1	1	0.22

The set of diagrams for producing the map of the zones at risk of pollution in the Baya basin is summarized by the flowchart of figure 2

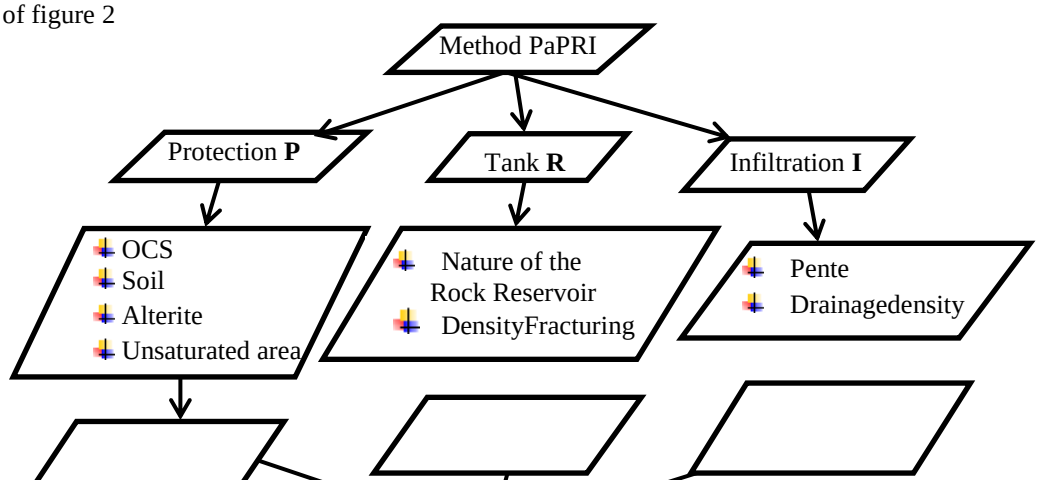

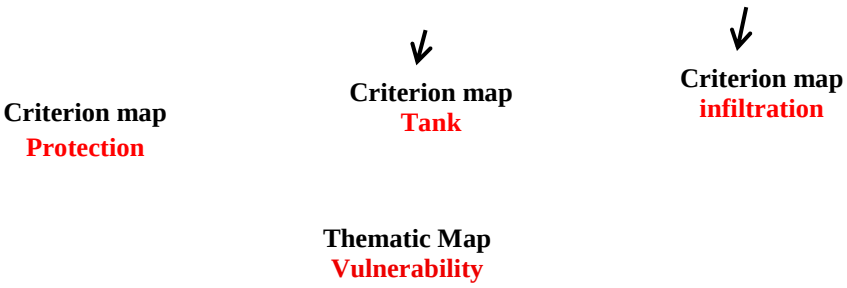

Figure 2 : Flowchart of the multi-criteria analysis for the production of the map of pollution risk areas

1.3. Validation of the vulnerability map

1.3.1. Calculation of the margin of error (Er) and expansion factor K

The calculation of uncertainties or margins of error on the thematic pollution susceptibility maps were determined according to Ehoussou et *al.*, (2018) and Mangoua et *al.* (2019) from Equation 2.

$$\mathrm{Er} = \frac{\sum \Delta\bar{X}}{Iv} Eq\ (2)$$

$\Delta\bar{X}$: Uncertainty on the average of each data series;
Iv: Global vulnerability index.
The uncertainty on each parameter is determined from equation 3 (Houria, 2007)

$$\Delta\bar{X} = \frac{\sigma}{\sqrt{m}} = \sqrt{\frac{1}{m(m-1)}\sum_{i=1}^{m}|(X_i - \bar{X})|^2} Eq\ (3)$$

σ: standard deviation; m: number of data; X_i: value of each parameter; $\bar{X}$: average of each data series.
An expansion factor (K) is calculated to determine the confidence level based on the statistical principle of uncertainty calculation. The expression of this factor is given by equation 32 (Mangoua et *al.*, 2019):

$$K = \frac{|E-\bar{X}|}{\sigma} Eq\ (4)$$

K is the expansion factor; E is the extreme value of the statistical series which may be the maximum or the minimum of this series. The confidence levels of the different parameters were deduced from the different values of K. Thus, K=1 for a confidence level of 68%; K=2 for a confidence level of 95% and K=3 for a confidence level of 99%.

1.3.3. Validation of maps by nitrates

The validity of the pollution vulnerability map obtained by the PaPRI methods was tested by nitrate concentrations according to the work of Allechy et *al.* (2016) and Mangoua et *al.* (2019). The selection of nitrates (Table 2) as an indicator of vulnerability is due to the fact that these ions are stable, soluble, mobile and readily reach groundwater (Bonton et *al.*, 2010).

Table 2 : Localities with NO_3^- levels above the WHO guideline (2017)

Locality	Siédja	Agnibilekro	Kwassia-nangrin	Tiédo	WHO (2017)
X coord	492395	474140	496050	468667	-
Y coord	855807	783904	816652	871727	-
NO_3^-(mg.L^{-1})	109,6	110,8	79,5	56,7	50

The high concentration of nitrates detected in groundwater by N'Guettia (2023) in 2007 is 29 mg.L^{-1}, that of 2016 and 2017 are respectively 109.6 and 193.7 mg.L^{-1}. Indeed, 25% of the waters sampled in 2017 have nitrate concentrations higher than the WHO directive (2017) which is 50 mg.L^{-1} for nitrate.

2. Results

2.1. Pollution susceptibility map

The combination of all the criteria protection, reservoir rock and infiltration made it possible to obtain the vulnerability map by the PaPRI method from the scenario where the weighting coefficient of the protection criterion is the highest (0.71), then the reservoir rock criterion (0.22), infiltration criterion (0.06). When analyzing this map (FIG. 43), four (4) classes of vulnerabilities are highlighted. The very strong vulnerability class with 32% proportions. The low, middle and high vulnerability classes occupy 12%, 31% and 25% of the total area of the basin, respectively. The strong and very strong classes are distinguished in the center in the localities of Tanda and Koun-fao, in the southeast, in the localities of Tankéssé, Agnibilékrou and Akobouassué and finally, in the east, in the localities of Transua and Assuéfry. Islets of plots stand out on the western flank and in the north of Tabagne. Areas with average vulnerability to pollution occupy about 31% and well-protected land in the basin accounts for 12%. The basin susceptibility map has a margin of error of ± 0.004 with a confidence level of K = 1.71 or 95%.

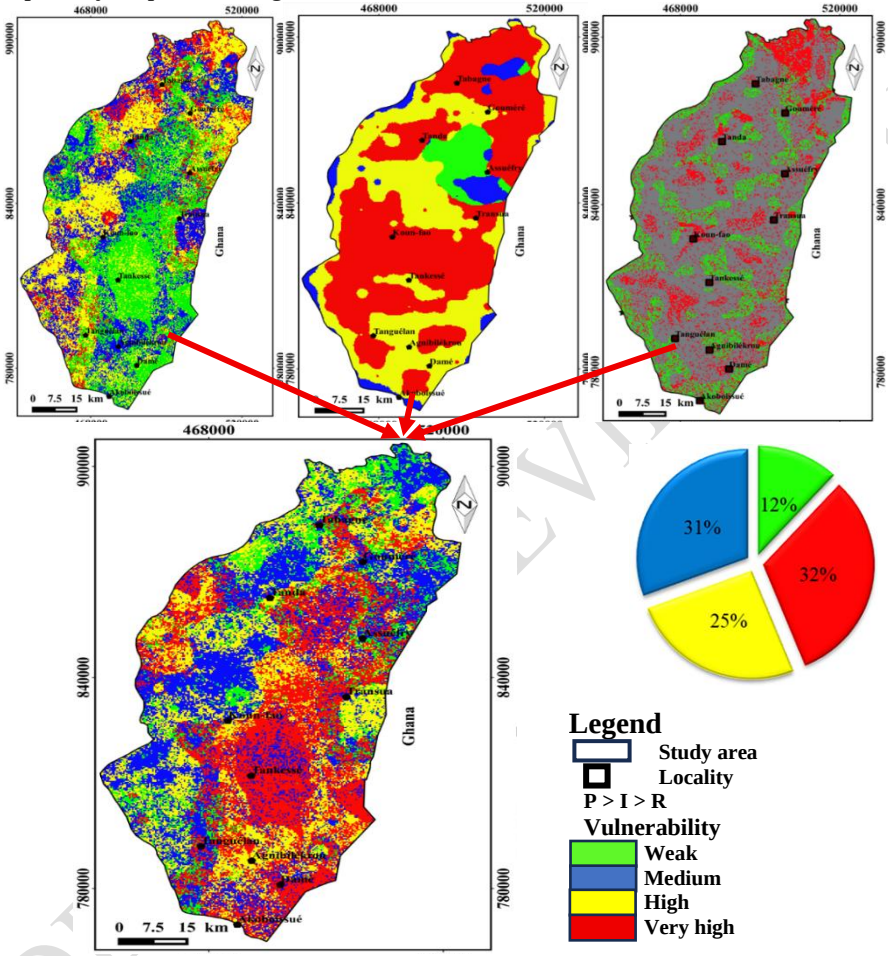

Figure 3 : Vulnerability map and distribution diagram of basin pollution susceptibility classes

2.2. Distribution of nitrate concentrations according to pollution susceptibility zones

The pollution vulnerability map was validated using nitrate (NO_3^-) levels obtained during the various sampling campaigns. The concentrations contained in the boreholes are between 0.4 and 109.6 mg. L^{-1}. Those contained in the wells vary between 0.8 and 193.7 mg.L^{-1}. Indeed, out of a total of 74 groundwater samples (50 boreholes, 24 wells), 59 or 74.52% contain traces of nitrates. Of these, 7.59% have levels below the WHOrecommended drinking water threshold value (50 mg.L^{-1}).

Concentrations between 10 and 50 mg.L-1 represent 46.83% of the water samples. The spatial distribution of these contents on the pollution susceptibility map is illustrated in FIG. 58. The percentages recorded by vulnerability class are random from one class to another (Table XXX). Areas with a high and very high risk of nitrate pollution represented by yellow and red, i.e. 57% of the total area of the basin, coincide with areas with high human densities. The nitrate concentrations obtained in the Siédja drilling (109, 6mg.L-1), in the Tiédo (110, 8mg.L-1), Kwassia-nanguinin (79, 5mg.L-1) and Agnibilékrou (56, 7mg.L-1) wells are recorded in urban areas. Concentrations were

also recorded in agricultural areas, such as the Yaokroko well and N'djorekro, which recorded a concentration of 10.3 and 0.8 mg.L-1, respectively.

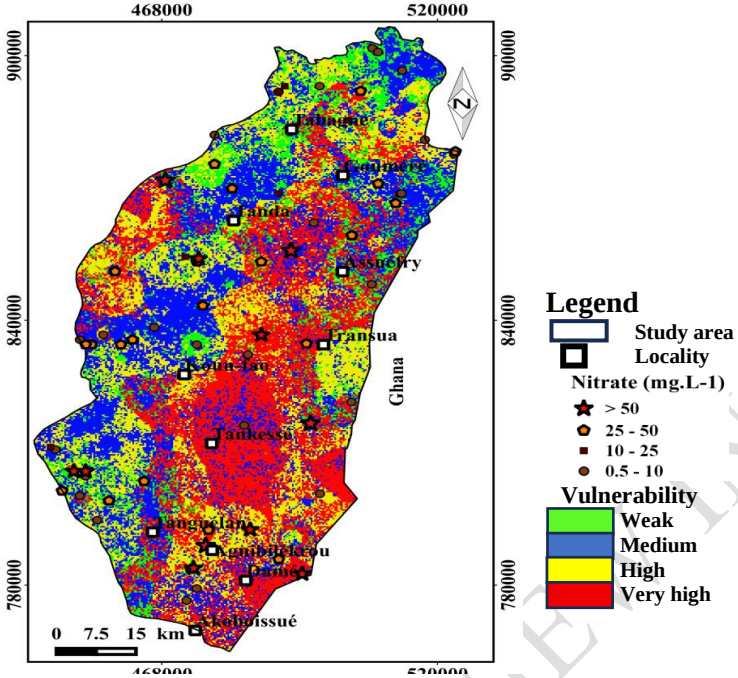

Figure 4 : Distribution of nitrate contents on the vulnerability map

Table 3 : Classification of nitrate levels by vulnerability

Classe	*% vulnerability class*	*% coincidence rate*	*Class of nitrate (mg. L^{-1})* **Number and percentage of sample**			
Indices	*P > I > R*	*Nitrate*	*0 - 10*	*10 - 25*	*25 - 50*	*> 50*
Weak	*6,04*	21,81	5/ 13,8%	3 / 42,9%	2 / 10%	-
Medium	*16,17*	*58,18*	*10/ 27,8%*	*4/ 57,1%*	*5/ 25%*	*2/ 18,2%*
High	*62,5*	*12,72*	*17/ 47,2%*	*1/ 14,3%*	*8/ 40%*	*4/ 36,4%*
Very high	*15,52*	*7,27*	*4/ 23,5%*	-	*5/ 25%*	*5/ 45,5%*

3. Discussion

Mapping groundwater vulnerability is considered by Amharref and Bernoussi (2007) as a decision-making tool, since it helps to guide land use planning and preserve the health of populations. The mapping of vulnerability to aquifer pollution in the Baya watershed has yielded four distinct vulnerability classes; a low vulnerability class where the aquifer appears to be protected (12%); a medium vulnerability class (31%); a high vulnerability class (25%) and a very high vulnerability class (32%).This result indicates potential contamination risks, which could be explained by the fact that these areas are densely fractured with low weathering thicknesses where strong slopes coexist (Mangoua, 2013). These areas are considered areas to be monitored. Indeed, just like the PaPRIKa method, in accordance with the concepts of Mangin (1975) developed for karsts, the PaPRI method has shown that the basin remains dominated by strong and very strong vulnerability classes, i.e. 57% of the total area of the basin.This high vulnerability could be linked on the one hand to the strong anthropization of these surfaces and on the other hand to the depth of the aquifer (less than 1m in places during the rainy season). Indeed, according to Mejia et *al.* (2007), the depth of the slick determines the distance that the pollutant must travel before reaching the slick. The lower the water level relative to the ground, the faster the pollutant could reach the water table (Dibi et *al.*, 2013). Field investigations have shown that the strong and very high pollution susceptibility classes correspond to urban areas and agricultural plots (rubber trees, cocoa, coffee, cashew, vegetable gardens, etc. (N'Guettia, 2023). This vulnerability is reinforced by the presence of septic tanks in urban areas. Similar results of vulnerability to pollution were obtained by Mejia et *al.* (2007), Dibi et *al.* (2013), Koudou et *al.* (2016) and Lunga (2017). This situation justifies the high vulnerability of the water table to pollution observed in urban areas and agricultural plots in the basin (N'Guettia,2023). Also, the strong and very strong susceptibility classes coincide with that of the potential

map of the basin(Mangoua 2013). Indeed, Kouadio (2019) , these areas would be favorable to the recharge of the basin's water table. The vulnerability of these areas could also be explained by the presence of low slopes observed in most of these areas. Indeed, the degree of slope determines the infiltration power of the runoff. The steeper the slope, the weaker the runoff and the more water is able to infiltrate (Ahmed, 2009; Bentekhici et *al.* (2018). The PaPRI method has given good results in this work as shown in the work of Dibi et *al.* (2015), Mangoua et *al.* (2019). it is therefore possible to define the sensitive areas in which pollution can seriously affect a slick and to have an idea of the means to be used if we want to protect this slick. The pollution vulnerability map was validated using nitrate contents. Several studies on similar topics have produced the same results.Indeed, studies by Aké (2020), Zhou et *al.* (2016); Kouadio (2018) and Mangoua (2019) have shown that water vulnerability is best expressed by the nitrate-specific vulnerability method. Thus, the projection of the water points on the pollution susceptibility map gave a coincidence rate of 81.13%. In all cases, the areas actually contaminated correspond to localities with high human densities and agricultural parcels.

4. Conclusion

The combination of GIS and multi-criteria analysis by the PAPRI method allowed the realization of the vulnerability map of the Baya watershed. This map presents four (4) vulnerability classes (low (12%), medium (31%), high (25%) and very high (32%) which briefly describe the areas of susceptibility to pollution in the basin.The basin has areas with a high susceptibility to pollution with strong and very strong classes that correspond to urban, agricultural and poultry plots. This vulnerability map has circumscribed the areas sensitive to pollution, 57% of which require protection. The map with a confidence level of around 95% is an important and indispensable source of information in that it provides an accurate picture of the pollution sensitive areas with a view to taking the necessary protective measures.

5. References

1 Allechy F.B., Lasm T. (2016). Mapping Of The Vulnerability To Pollution Of The Aquifers Of The Precambrian Base: Case Of The Oumé Region (Central-West Côte D'Ivoire) European Scientific Journal, 12: 374- 391. DOI: http://dx.doi.org/10.19044/esj.

2 Ake G.E., Kouadio B.H., Kouadio K.C., Dongo K., Biemi J. (2020). Comparative Analysis Of The Mapping Of The Vulnerability To Pollution Of Fissured Aquifers In Agboville De partment By Drastic And SI Methods (South-East Of Côte d'Ivoire), European Scientific Jour nal, 16(24) : 312-335. Doi:10.19044/esj.2020.v16n24p312.

3 Ahmed M., Ji M., Qin P., Gu Z., Liu Y., Sikandar A., Iqbal MF. (2009). Javeed A. Phytochemical screening, total phenolic and flavonoids contents and antioxidant activities of Citrullus colocynthis L. and Cannabis sativa L. Applied ecology and environmental research 17(3): 6961-6979. DOI: http://dx.doi.org/10.15666/aeer/1703_69616979.

4 Amharref M., Aassine S., Bernoussi A.S., Haddouchi B.Y. (2007). Mapping vulnerability to groundwater pollution: Application to the Gharb plain (Morocco) Water Science Review. 20(2): 163-250.

5 Bentekhici N., Benkesmia Y., Berrichi F., Bellal S.A. (2018) Risk assessment of water pollution and vulnerability of the alluvial water table using spatial data. Case of the plain of sidi bel abbès (northwest algeria). Water Science Review, 31(1): 43-59.

6 Bonton. A., Rouleau A., Bouchard C., Rodriguez J.M. (2010). Assessment of groundwater quality and its variations in the capture zone of à pumping well in an agricultural area. Agricultural Water Management,97 : 824-834.

7 Dibi B., Kouassi K.L., Kouamé K.I, Konan K.S., Soumahoro M., Konan-waidhet A.B., Gnakri D. (2013). Assessment of vulnerability to pollution of aquifers of weatheredlayer by DRASTIC and SYNTACS methods: Case of M'Bahiakro city, Central Côte d'Ivoire", *International Journal of Innovation and Applied Studies.* 2(4): 464-476.

8 Dovonou F.E., Alassane A., Adjahossou V.N., Agbodo B., Djibril R., Mama D. (2017). Impacts of autonomous sanitation on well water quality in the Commune of Sèmè Podji (South Benin) International Journal of Biology Chemistry of. Science. 11(6): 3086-3099. DOI.org/10.4314/ijbcs. v11i6.42.

9 Ehoussou K.M., Kouassi A.M., Kamagate B. (2018). Hydrodynamic characterization of the aquifers fissured of the area of the "belier" (Center of Ivory Coast), Larhyss Journal, n° 36, pp. 119-143.

10 I.N.S. (2014). National Institute of Statistics, General Population and Housing Census. www. ins.ci., 25-47.

11 Humphries MS., McCarthy TS., Pillay L. (2017). Attenuation of pollution arising from acid mine drainage by a natural wetland on the Witwatersrand. *South African* journal *of* science. 113(12) : 1-9. DOI.org/10.17159/ sajs.2017/20160237.

12 Kouadio A.N.B. (2019) Assessment of the health risk associated with the consumption of traditional well water by low-income households in urban areas: case of the city of Agboville (Côte d'Ivoire), p188.

13 Koudou A., Adiaffi B., Assoma T.V., Sombo A.P., Amani M.E., Biemi J. (2013). Design of a decision support tool for groundwater prospecting in the basement area of south-eastern Côte d'Ivoire. Geo-Eco-Trop., 37(2): 211-226.

14 Lunga Z.R. (2017). Environmental impacts of anthropogenic pressure on the natural resources of the KAHUZI BIEGA National Park (PNKB) in the Province of South Kivuen R.D.Congo. CONGO SCIENCES, 5(1): 77-86. DOI: www.congosciences.org.

15 Mangin A. (1975). Contribution to the hydrodynamics of karst aquifers Contributions to the hydrodynamics of karst aquifers. Thesis, Dijon University (France), 124p.

16 Mangoua MJ. (2013). Assessment of the potential and vulnerability of groundwater resources in the aquifers fissures of the Baya watershed (eastern Côte d'Ivoire). Doctoral thesis. Nangui Abrogoua University, Abidjan (Ivory Coast), 171p.

17 Mangoua M.J., yao A.B., Douagui G.A., Kouassi K.A., Goula B.T.A., Biemi J. (2019). Assessment of the groundwater potential of cracked aquifers in the Bandama watershed (Ivory Coast), larhyss journal, 37: 53-74.

18 Mejia J. A., Rodriguez R., Armienta A., Mata E., Fiorucci A., (2007). Aquifer Vulnerability Zoning, an Indicator of Atmospheric Pollutants Input Vanadium in the Salamanca Aquifer, Mexico. Water,Air, Soil Pollution. 185: 95-100. DOI:10.1007/s11270-007-9433-x.

19 N'Guettia (2023). Dynamics of land use and physico-chemical quality of groundwater resources in the Baya watershed (Eastern Côte d'Ivoire), 150P.

20 SAEFL/SAEFL (2003) Delineation of groundwater protection areas in a cracked environment. Practical Guide, 83P.

21 OMS. (2017). Guidelines for drinking-water quality : 4th edition incorporating first adden dum. ISBN 978-92-4-254995-9, 538 p.

22 Tekam D.D., Vogue N., Nkfusai C.N., Ela M.E., Cumber S.N. (2019). Access to drinking water and sanitation: case of Douala V district commune (Cameroon), Pan African Medical Journal, 33(244): 1-8. DOI: 10.11604/pamj. 2019.33.244.17974.

23 UNICEF (2017). Progress in drinking water supply, sanitation and hygiene and SDG estimates, pp108. www.washdata.org.

24 Wang J., Liu G., Liu H., Lam P.K.S. (2017). Multivariate statistical evaluation of dissolved trace elements and a water quality assessment in the middle reaches of Huaihe River, Anhui, China. Science of the Total Environment. 583 : 421-43.

25 Youan Ta M., Yao K.A.F., Bakar D., De Lasmz. O., Lasm T., Adja M.G., Kouakou S., Onetie Z.O., Jourda J.P.R., Biemi J. (2015). Mapping of potential areas for the implantation of large-flow boreholes in a crack environment by multicriteria analysis: Case of the department of Oumé (west-central Côte d'Ivoire), Larhyss Journal, 23:155-181.

26 Yves S., Delor C., Zeade Z., Kone Y., Yao B.D., Vidal M., Diaby I., Konan G., Irié D.B., N'da D., Dommanget A., Cautru J.P., Guerrot C., Chiron J.C. (1995). Geological Map of Ivory Coast at 1/200 000 ; Agnibilekrou leaf. Memorandum from the Directorate of Mines and Geology, n°8, Abidjan, Ivory Coast, 19p.

27 Zhou P., Huang J., Pontius J.R.G., Hong H. (2016). New insight into the correlations between land use and water quality in a coastal watershed of China: Does point source pollution weaken it? *Science of the Total Environment,* 543 : 591-600. Doi.org/10.1016/j.scitotenv.2015.11.063